IEEE Access
Multidisciplinary ⋮ Rapid Review ⋮ Open Access Journal

Received 26 August 2022, accepted 4 September 2022, date of publication 8 September 2022, date of current version 16 September 2022.

Digital Object Identifier 10.1109/ACCESS.2022.3205109

RESEARCH ARTICLE

Impulse Noise Mitigation by Time-Diversity Hermitian Symmetry in Hybrid Powerline and Visible Light Communication Systems

MULUNDUMINA SHIMAPONDA-NAWA[1,2], OLUWAFEMI KOLADE[1,3], JIANHUA HE[4], (Senior Member, IEEE), WENBO DING[5], (Member, IEEE), AND LING CHENG[1], (Senior Member, IEEE)

[1]School of Electrical and Information Engineering, University of the Witwatersrand Johannesburg, Braamfontein, Johannesburg 2000, South Africa
[2]Faculty of Engineering and Built Environment, Wits Mining Institute, University of the Witwatersrand Johannesburg, Braamfontein, Johannesburg 2000, South Africa
[3]Department of Meteorology, University of Reading, RG6 6UR Reading, U.K.
[4]School of Computer Science and Electronic Engineering, University of Essex, CO4 3SQ Colchester, U.K.
[5]Tsinghua-Berkeley Shenzhen Institute, Tsinghua University, Shenzhen 518055, China

Corresponding author: Ling Cheng (ling.cheng@wits.ac.za)

This work was supported in part by the National Research Foundation of South Africa under Grant 148765, Grant 132651, and Grant 129311; in part by the Mwalimu Nyerere African Union (AU) Scholarship Scheme, SITA Aero; in part by the Department of Science and Innovation, South Africa. via the Mandela Mining Precinct (MMP); and in part by the European Union's Horizon 2020 Research and Innovation Programme through the Marie Skodowska-Curie Grants COSAFE under Agreement 824019 and VESAFE under Agreement 101022280.

ABSTRACT Hybrid powerline and visible light communication (HPV) systems offer a cost-effective method of providing high-speed communication in indoor and outdoor environments, for the realisation of internet of things (IoT). However, in the HPV system the powerline communication (PLC) channel is inherently susceptible to impulse noise (IN) due to electrical appliances randomly connected to the powerline. This adversely affects the HPV system's bit error rate (BER) performance. In this paper, a time-diversity Hermitian symmetry (TDHS) scheme, which mitigates the effects of IN in a PLC channel is proposed. The scheme employs the Hermitian symmetry structure to recover information symbols likely to have been affected by the IN. By using the TDHS scheme, the probability of the effect of IN on data symbols through a PLC channel, is drastically reduced by 75%. By simulations, the effectiveness of the TDHS scheme is demonstrated via the enhanced BER performance of the system. The TDHS scheme is then implemented over a permutation coded HPV system using the amplify-and-forward protocol at the PLC-VLC integration unit and the Hungarian-Murty (HM) soft-decision decoder at the destination. The combination of the TDHS scheme and the HM decoder in a coded system provides further BER performance enhancement, exceeding 10 dB gain in signal-to-noise ratio (SNR) at a BER of 10^{-4}.

INDEX TERMS Hermitian symmetry, hybrid powerline and visible light communication, impulse noise, time-diversity.

I. INTRODUCTION

Smart homes, smart cities, smart mines, wearables and connected cars are just but a few areas where the internet of things (IoT) has developed and will continue to grow [1], [2], [3]. This growth demands increasingly wide coverage areas, high capacities and data rates to maintain reliable and ubiquitous connectivity of several smart devices and machines, regardless of their environment and geographical locations. Thereby presenting a challenge on the current commonly used standalone radio frequency (RF) networks. Therefore, hybrid networks where various communication technologies complement each other to achieve the device-to-device and device-to-infrastructure connectivity, have been proposed [3], [4], [5], [6], [7], [8]. Some of the common communication technologies studied for hybrid networks include RF, visible light communication (VLC) and powerline communication (PLC). VLC is a type of optical wireless communication

The associate editor coordinating the review of this manuscript and approving it for publication was Fang Yang.

technology that uses the electromagnetic wavelengths within the visible spectrum. Thus, VLC is capable of providing illumination and data communication simultaneously. On the other hand, the powerline provides power to the VLC transmitters and also works as an information backbone [9], [10], [11], [12].

Fig. 1 depicts some areas where hybrid networks consisting of either a pair of or all of the three technologies previously mentioned, have been applied with potential for optimisation. For example, hospitals and underground mines have areas where an RF solution could be undesirable, thus VLC can be used as an access point solution, whose information is provided via the PLC channel. Fig. 1 also shows a smart transport system, where the RF and VLC technologies complement each other to achieve the vehicle-to-vehicle (V2V) and vehicle-to-infrastructure (V2X) communication involving traffic lights and security/speed cameras installed on the road. Furthermore, a hybrid of RF, PLC and VLC is assumed for achieving the smart home, shown in Fig. 1. Additionally, a hybrid configuration is shown for a smart car whose powerline network is integrated to its VLC enabled lights. All these scenarios show that hybrid networks are inevitable in achieving several simultaneous smart device connectivity.

The presence of the powerline in most locations of Fig. 1, makes PLC a strong candidate for championing the IoT campaign, for smart cities, smart underground mines and smart homes [3], [4], [5], [13]. Additionally, because high power efficient solid state lighting is being rolled out for both outdoor and indoor illumination, it is possible to have VLC wherever the installation of solid state lighting is available. Hence, VLC has also been proposed to be one of the main technologies that enable the full realisation of IoT [4], [14], [15]. Motivated by the relevance of both PLC and VLC in the IoT domain and the drive towards hybrid networks, in this work, we investigate the hybrid configuration of PLC and VLC, we refer to as the HPV system.

Since the first demonstration of VLC [10], [11], light emitting diodes became the highly considered VLC transmitters due to their advantages of low cost, energy efficient, durability and their ability to be modulated at high speed. Apart from the much desired wide unlicensed spectrum in order of several hundred terahertz (THz), some notable advantages attributed to VLC technology are its non-subjection to interference by electromagnetic sources, congestion, as well as high level of security since it does not penetrate through walls. Potential application areas for VLC include, but not limited to hospitals and mines where RF could be undesirable, smart transport systems, smart lighting of smart buildings and underwater communication.

Like VLC, PLC has an advantage of having ubiquitous presence in indoor environments which is a desirable communication network feature for coverage enhancement. Some of the applications of PLC include providing remote meter reading services, voice communication, data acquisition and intra-vehicle communication [5], [12], [13].

In light of the above, the integration of PLC and VLC is naturally achievable based on the fact that lighting devices always need power supply and that powerlines are ubiquitously available in environments such as houses, hospitals, office spaces, server rooms and high busy trading areas such as shopping malls [16], [17], [18]; resulting in a cost-effective implementation of the HPV system.

Being an emerging and developing integrated scheme, various areas of the HPV system still require optimisation. Hence, since the first demonstration of an HPV system [16], a significant number of studies with regards to integration schemes between PLC and VLC, hybrid channel models, coverage optimisation, modulation, multiplexing, multiple access (MA), as well as spectrum and power efficiency schemes, have been reported. For instance, simulated HPV channel models based on PLC and VLC practical measurements are presented in [19] and [20], while authors in [21] and [22] derived the HPV channel models using a semi-hidden Markov model (SHMM) with the aid of a Fritchman channel state representation model. Measurements obtained from different positions were used in an indoor VLC environment, aided by software-defined radios. Integration techniques of the two channels is also an area that has received a lot of attention, with the two main protocols identified as amplify-and-forward (AF) and decode-and-forward (DF) [22], [23], [24], [25]. For the AF protocol, the signal received from the PLC channel is scaled and amplified, before modulating the VLC transmitters. On the other hand, in the DF protocol, the signal is decoded and subjected to the AF processes before being re-transmitted by the VLC transmitters.

In [26] and [27], the bit error rate (BER) performance of an HPV system with multiple-input multiple-output (MIMO) configurations at the VLC sections, is presented with practical indoor considerations. It was established that channel effects from both PLC and VLC have an influence on the BER performance of the HPV system. Moreover, the location and positions of the transmitters and receivers at the VLC section also have an influence on the BER performance of the system. Furthermore, single carrier M-ary modulation schemes such as phase shift-keying, multi-carrier modulation such as orthogonal frequency division multiplexing (OFDM) and multiplexing schemes such as color shift-keying (CSK) and bit division multiplexing (BDM) have been investigated for HPV systems [25], [28], [29], [30]. Additionally, both orthogonal and non-orthogonal MA techniques have also been considered for the HPV system [31], [32], [33], demonstrating the hybrid scheme's potential to be used in high speed networks and ultimately, for IoT. With such significant ongoing research work, HPV systems are not only projected to complement, but in some application areas, projected to substitute the existing RF solutions.

II. PROBLEM STATEMENT AND MOTIVATION

Despite their merits, HPV systems are prone to channel noise. Precisely, in an indoor environment where electrical appliances are randomly plugged in the powerline, noise impulses

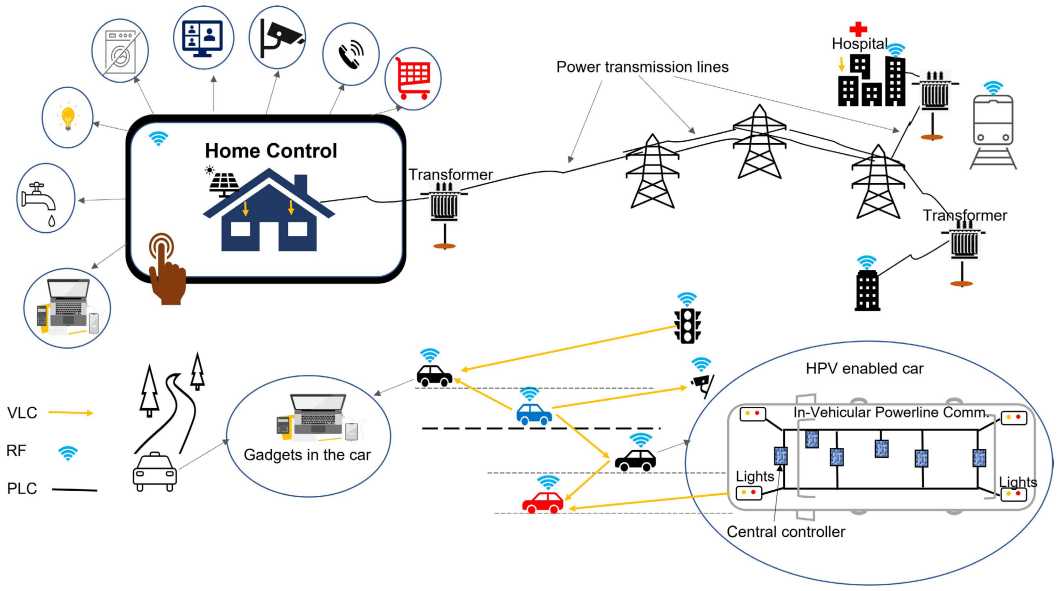

FIGURE 1. A depiction of hybrid networks of RF, PLC and VLC technologies for infrastructure and device interconnection.

are injected affecting the communication signals that are transmitted over the PLC channel. In literature, impulse noise (IN) has been shown to occur in random bursts [34], [35], [36], [37], [38], [39], [40], [41], affecting either a group of frequencies over a period of time or data symbols in a sequence of time-slots.

Several methods to combat the effects of IN and narrow-band interference (NBI) in the fast time-varying PLC channel have been proposed. For instance, the simple method of suppressing the IN effects by preceding the OFDM receiver with clipping or blanking [42] has been successfully applied in PLC systems to enhance the performance of the OFDM receiver [43], [44]. The work in [42] demonstrated that simultaneously exploiting the advantages of the clipping and blanking schemes by combining them yields better results, compared to using the two schemes independently. While, in [43], pre-processing the signal at the transmitter was proposed and shown to enhance the performance of the blanking/clipping-based techniques for IN mitigation in powerline channels. In [45], simple iterative impulsive noise suppression algorithms that exploit the noise structure in the time and frequency domain, were shown to improve the performance of the OFDM receiver. Further, in [44], the performance of the PLC system was enhanced by preceding the iterative algorithms discussed in [45] with a clipping and nulling technique. Noting the inherent issue of high peak-to-average power ratio (PAPR) of the transmitted signal in OFDM-based systems, various studies have proposed and used some variations of the OFDM techniques in PLC. For example, vector OFDM (VOFDM) has been reported to exhibit lower PAPR than conventional OFDM [46], [47], consequently resulting in an energy efficient PLC system. Others include the combination of OFDM with phase and continuous phase modulation (PM and CPM), which is referred to as constant envelope OFDM (CE-OFDM) [48], [49].

In addition to techniques mentioned above for mitigating IN and PAPR in OFDM based PLC systems, coding techniques have been exploited to address the issue of IN [50]. For instance, permutation codes (PCs) combined with a non-coherent detection scheme such as Mary frequency shift keying (MFSK), makes the communication system robust against permanent frequency disturbances and IN [50]. Whereas in [51], the use of MFSK was shown to mitigate the NBI noise and IN in fast time-varying channels. In addition, a combination of PCs and MFSK was proposed and shown to also mitigate the effects of the burst noise in PLC channels [52], [53], [54].

Time-diversity schemes have also been applied in different communication technologies for performance reliability enhancement [26], [38]. In time-diversity schemes, information bits or symbols are repeatedly transmitted such that the receiver has multiple copies of the transmitted signal, from which different decoding schemes such as maximum ratio combining (MRC), majority rule scheme or any comparison based technique, can be applied. In [38], a time-diversity permutation coding scheme for NBI powerline channels was proposed. In the proposed time-diversity scheme of [38], the same information symbol is repeatedly sent over the channel at different times to mitigate the effects of IN. Because the time between repeated information symbols is adjusted to be longer than the length of a typical error burst, then the probability of the repeated information symbol to be affected by the same burst error is reduced. Hence, the unaffected information symbol can be used to recover the transmitted signal.

In this work, a novel time-diversity scheme based on the Hermitian symmetry (HS) structure is proposed and implemented at the PLC section of the HPV system. The time-diversity scheme aims at improving the overall BER performance of an HPV system by mitigating the effects

of IN in the PLC channel. Unlike the schemes discussed above that exploit the noise structure in the channel or the effects of the employed modulation techniques to mitigate the IN, in this work, we exploit the HS, a fundamental signal property, that has commonly been used to generate real OFDM signals in optical systems. In a cascaded system like HPV, the achieved data rate is proportional to the data rate of the constituent technology with the lower data rate capability. Thus, the use of the HS structure at the PLC section, which is twice that of the conventional system does not in any way affect the system data-rate. Moreover, in this work where optical OFDM is applied at the VLC section, the HS structure is required to ensure that the signals to modulate the VLC transmitters are intensity-modulation direct-detection (IM/DD) compatible. Therefore, the TDHS scheme with an enhanced reliability, offers the same data rate capability as the conventional system because of the HS constraint at the integration unit. By conventional HPV system, we refer to the system where the information symbols are transmitted without being subjected to the HS structure, at the PLC section. Furthermore, the proposed TDHS scheme uses the AF relaying protocol. Consequently, the implementation is simplified and less complex in comparison to an integration unit using the DF relaying protocol.

Since IN occurs in short bursts and can affect data symbols in sequence of time-slots, then a scheme that only activates a selected and spaced number of time-slots to carry information would further enhance the system's BER performance. As such, PCs are used to attain a systematic pattern of time-slot activation. We note from literature that PCs can be used in an MA system to identify different users [50], [55], hence the TDHS scheme with PCs is extended to an MA HPV system. We also note that the MA schemes in literature are mostly applied to the VLC section of the HPV system only. However, in this work, by using PCs, we apply the MA scheme at the PLC section and show that the message can be correctly decoded at the VLC receiver, while the need for decoding at the PLC/VLC unit is eliminated. While most of the IN mitigation schemes mentioned above focus on application of the IN mitigation schemes to multi-carrier modulated signal in the PLC channel, the TDHS scheme can be applied to both single and multi-carrier modulated signals.

Precisely, the contributions of this work can be summarised as follows:

- Design and investigation of a novel time diversity scheme based on the Hermitian symmetry to effectively mitigate the inherent IN in PLC channels.
- We then propose a permutation coded TDHS system and use a soft-decision (SD) decoder based on the Hungarian and Murty's optimisation algorithms, for further performance enhancement.
- Unlike most literature on HPV systems where the MA scheme is implemented at the VLC transmitter section, we extend the permutation coded TDHS scheme to an MA system implemented from the PLC transmitter section.
- We provide an analysis of the performance of the proposed TDHS scheme, in terms of BER and goodput, and further compare the results of the HPV system using the TDHS scheme to the results of the conventional HPV systems using both AF and DF protocols.

The rest of the paper is organised as follows: Section III gives the details of the TDHS-based HPV system model as well as the permutation coded TDHS (PC TDHS) system. Under the PC TDHS subsection, the decoding process of the applied SD HM decoder is also presented. Additionally, the principle of the IN detector used at the PLC/VLC integration unit is described. The final part of Section III introduces an MA scheme implemented as an extension of the permutation coded TDHS system. In Section IV, the details of the conducted simulations and results analysis of the investigated systems are presented, after which a conclusion is provided in Section V, the final section of this paper.

III. TIME DIVERSITY HERMITIAN SYMMETRY BASED HPV SYSTEM MODELS

An HPV system where a single carrier modulation (SCM) scheme is implemented in the PLC section while a multi-carrier modulation scheme, precisely OFDM, is implemented at the VLC section, is considered. The use of an SCM in the PLC section avoids the complexity of the use of the fast Fourier transform (FFT) and its inverse at the PLC/VLC integration unit and PLC input, respectively. To reduce the system's complexity due to the decoding process at the integration unit, the AF relaying protocol is employed.

A. TDHS BASED HPV SYSTEM

1) SYSTEM MODEL OVERVIEW

In the investigated TDHS-based HPV system, the structure of the HS is exploited as a time-diversity mitigation method against IN in the PLC channel. $\frac{N}{2}-1$ information symbols are transmitted from the PLC side in each transmit period; N is the length of the HS window. The $\frac{N}{2}-1$ symbols are arranged in an HS structure before they are transmitted over the PLC channel, such that, a message symbol x_n is duplicated in the form of its complex conjugate x_n^*, for $n = 2, 3, \ldots, \frac{N}{2}$, where the superscript $*$ denotes the complex conjugate. For N time-slots, the general expression relating the message symbols, their complex conjugate and their positions due to the HS constraint is given as:

$$x_{(\xi+2)} = x^*_{(N-\xi)}, \quad \xi = 0, 1, 2, \ldots, \frac{N}{2} - 2. \tag{1}$$

Thus, the HS structure is formed by concatenating the original vector of message symbols with the vector of their complex conjugate symbols as, $[0, x_2, x_3, \ldots, x_{(\frac{N}{2})}, 0, x^*_{(\frac{N}{2})}, \ldots, x^*_3, x^*_2]$. Equivalent symbols, x_n and x_n^*, are therefore separated enough to avoid the effect of IN which occurs in short bursts. The first and $(\frac{N}{2}+1)^{\text{th}}$ components in the HS structure are set to zero, to avoid any direct-current (DC) shift or residual complex component in the time domain signal.

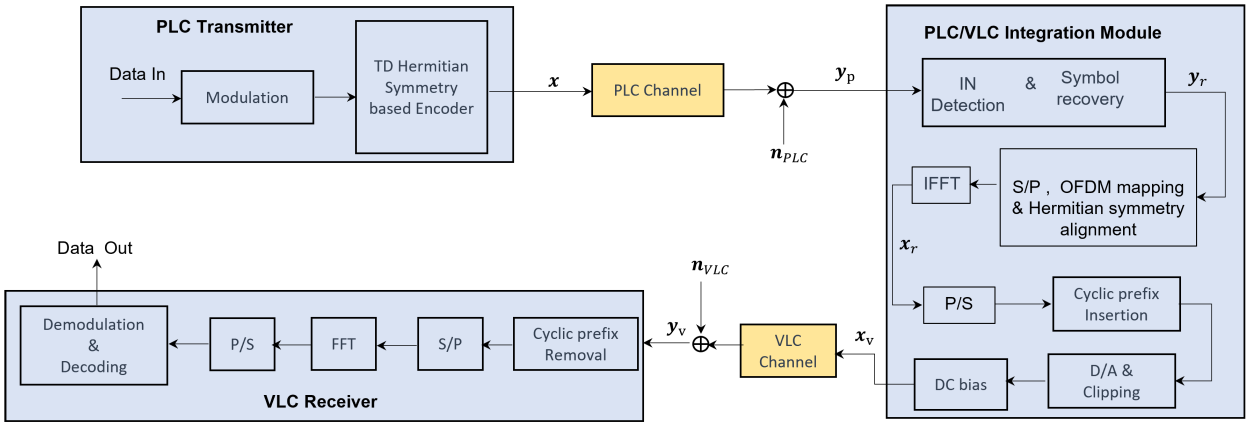

FIGURE 2. Block diagram of the TDHS based HPV system. D/A, P/S and S/P represent the digital-to-analog, parallel-to-serial and serial-to-parallel processes, respectively.

As shown in Fig. 2, the transmitted signal is affected by the noise in the PLC channel. Hence, the output signal vector, $\boldsymbol{y}_{\mathrm{p}}$, from the PLC channel is given as

$$\boldsymbol{y}_{\mathrm{p}} = \boldsymbol{x}e^{j\phi} + \boldsymbol{n}_{\mathrm{p}}, \tag{2}$$

where p is used to denote the signals in the PLC section. In (2), $\boldsymbol{x} = [0, x_2, x_3, \ldots, x_{(\frac{N}{2})}, 0, x^*_{(\frac{N}{2})}, \ldots, x^*_3, x^*_2]$ denotes the complex input message symbols in the HS window, transmitted via the PLC channel. The output signal vector, $\boldsymbol{y}_{\mathrm{p}} = [y_{\mathrm{p1}}, y_{\mathrm{p2}}, y_{\mathrm{p3}}, \ldots, y_{\mathrm{p}(\frac{N}{2})}, y_{\mathrm{p}(\frac{N}{2}+1)}, y^{\dagger}_{\mathrm{p}(\frac{N}{2})}, \ldots, y^{\dagger}_{\mathrm{p3}}, y^{\dagger}_{\mathrm{p2}}]$. Due to the effect of the PLC noise on $\boldsymbol{x}$, the complex conjugate feature does not hold for $\boldsymbol{y}_{\mathrm{p}}$. However, the position of the elements in the received vector are still assumed. Thus, to differentiate the elements from the complex conjugate notation, the superscript, † is used. In addition, $\boldsymbol{n}_{\mathrm{p}} = \boldsymbol{n}_{\mathrm{G}} + \boldsymbol{n}_{\mathrm{I}}\sqrt{D}$ denotes the noise component in the PLC channel comprising the background noise $\boldsymbol{n}_{\mathrm{G}}$ and the IN, $\boldsymbol{n}_{\mathrm{I}}$. The background noise is modelled as additive white Gaussian noise (AWGN) (a complex component with zero-mean and variance of $\sigma^2_{\mathrm{G}} = 2N_0$, where N_0 is the noise power spectral density) and IN is assumed to have a Poisson distribution with a variance σ^2_{G}/A. A is the impulsive index determining the frequency of occurrence of $\boldsymbol{n}_{\mathrm{I}}$ and D is a variable imposing the Poisson distribution on $\boldsymbol{n}_{\mathrm{I}}$.

The signal received from the PLC channel is passed to the IN threshold detector (see Section III-A2) where, if a transmitted symbol, $y_{\mathrm{p}(n)}$, was affected by IN, then the appropriate symbol amplitude is recovered from the element, $y^{\dagger}_{\mathrm{p}(n)}$. It should be noted that elements in the first and $(\frac{N}{2}+1)^{\mathrm{th}}$ positions of $\boldsymbol{y}_{\mathrm{p}}$ are basically noise components since zeros were transmitted in these positions. Thus, there are $\frac{N}{2}-1$ recovered complex symbols on which OFDM will be applied. We denote the vector of these recovered symbols as $\boldsymbol{y}_{\mathrm{r}}$. Precisely, if the zero that was transmitted in the first position is included and occupies the first position again, then $\boldsymbol{y}_{\mathrm{r}} = [0, y_{\mathrm{r2}}, y_{\mathrm{r3}}, \ldots, y_{\mathrm{r}(\frac{N}{2})}]$.

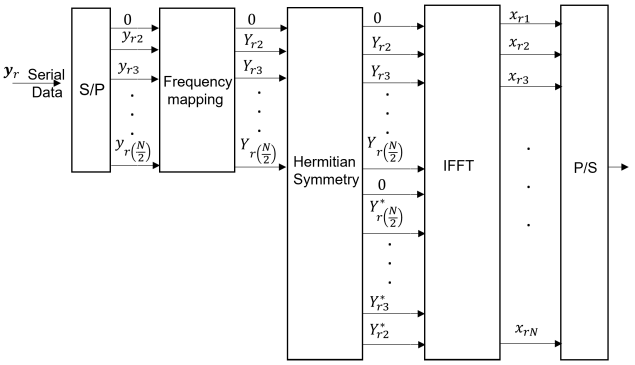

FIGURE 3. Block diagram showing the signal output from the S/P, OFDM mapping & Hermitian symmetry alignment and the IFFT blocks of Fig. 2.

In this work, IM/DD is employed, as such, the OFDM signal modulates the current of the VLC transmitter and a photo-detector is used for detection, at the receiver. To ensure IM/DD compatibility and obtain real OFDM signals, frequency symbols to which $\boldsymbol{y}_{\mathrm{r}}$ is mapped, are forced to satisfy the Hermitian symmetry constraint (1), before the inverse fast Fourier transform (IFFT) is performed, as depicted in Fig. 2. An expansion of the S/P, OFDM mapping & Hermitian symmetry alignment block of Fig. 2, is shown in Fig. 3, with details of the processed signal from each stage. The frequency domain signal $\boldsymbol{Y}_{\mathrm{r}}$, at the input of the IFFT block is expressed as $[0, Y_{\mathrm{r2}}, Y_{\mathrm{r3}}, \ldots, Y_{\mathrm{r}(\frac{N}{2})}, 0, Y^*_{\mathrm{p}(\frac{N}{2})}, \ldots, Y^*_{\mathrm{r3}}, Y^*_{\mathrm{r2}}]^{\mathrm{T}}$; where the function $[.]^T$ denotes vector transposition.

The bipolar real-valued, time domain symbols obtained after the IFFT block are serially aligned and can be expressed as $\boldsymbol{x}_{\mathrm{r}} = [x_{\mathrm{r1}}, x_{\mathrm{r2}}, x_{\mathrm{r3}}, \ldots, x_{\mathrm{r}N}]$. The cyclic prefix (CP) is then added to $\boldsymbol{x}_{\mathrm{r}}$ for inter-carrier and inter-symbol interference mitigation, after which, DC biasing is applied to achieve the uni-polar signals required to modulate the current of the VLC transmitters. We denote the signal from the VLC transmitters as $\boldsymbol{x}_{\mathrm{v}}$, where v is specifically used to denote the signals in the VLC section. Thus, $\boldsymbol{x}_{\mathrm{v}}$ is transmitted by the VLC

transmitters having a Lambertian radiation pattern influenced by the channel gain element, h, between the transmitting LED and the corresponding receiving photo-diode. Consequently, the received signal at the VLC receiver can be expressed as:

$$\boldsymbol{y}_{\mathrm{v}} = h\boldsymbol{x}_{\mathrm{v}} + \boldsymbol{n}_{\mathrm{v}}, \tag{3}$$

where the AWGN affecting the received optical signal is denoted by $\boldsymbol{n}_{\mathrm{v}}$ and h is approximated as [56],

$$h = \begin{cases} \frac{A_{\mathrm{r}}(\ell+1)}{2\pi d_{\mathrm{v}}^2} cos^{\ell}(\alpha) cos(\psi), & 0 \leq \psi \leq \Psi_c \\ 0 \quad \text{elsewhere.} \end{cases} \tag{4}$$

In (4), A_{r} is the effective collection area of the detector located at a distance of d_{v} from the transmitter. The detector's angle of irradiance with respect to the transmitter is denoted as α, while the angle of incidence is denoted by ψ. The Lambertian emission order is given by $\ell = \frac{-\ln 2}{\ln(cos\Phi_{1/2})}$, where $\Phi_{1/2}$ is the semi-angle at half power of the transmitter.

At the VLC receiver, the analogue signal is converted to digital signal, the CP is removed and the serial sequence is converted to parallel sub-carriers, after which the FFT is performed on the received signal. Demodulation and decoding then follow, to recover the transmitted signal. We assume that the receiver has a perfect knowledge of the channel. Hence, maximum likelihood detection is used to estimate the likely transmitted message symbols. Therefore, the $\hat{\boldsymbol{x}}_{\mathrm{v}}$ which minimises the Euclidean distance between the actual received signal vector, $\boldsymbol{y}_{\mathrm{v}}$ and all potential received signals, is accepted as the transmitted vector and is expressed as:

$$\hat{\boldsymbol{x}}_{\mathrm{v}} = \arg\min_{\boldsymbol{x}_{\mathrm{v}}} ||\boldsymbol{y}_{\mathrm{v}} - h\boldsymbol{x}_{\mathrm{v}}||_{\mathrm{F}}^2, \tag{5}$$

where $||.||_{\mathrm{F}}$ denotes the Frobenius norm.

2) IN DETECTION

At the PLC channel output, a simple IN threshold detector which compares the magnitudes of $y_{\mathrm{p}(n)}$ and $y^{\dagger}_{\mathrm{p}(n)}$, is used to determine whether an information symbol was affected by IN. In this work the threshold, θ, is assumed to be five times the average transmitted power. The component between $y_{\mathrm{p}(n)}$ and $y^{\dagger}_{\mathrm{p}(n)}$, with a lower magnitude with respect to (wrt) θ, is assumed to be the symbol that was not affected by IN and is selected for re-transmission by the VLC transmitter. Thus, for $n = 2, 3, \ldots \frac{N}{2}$, the symbol to be transmitted must satisfy

$$y_{\mathrm{r}(n)} = \min(y_{\mathrm{p}(n)}, y^{\dagger}_{\mathrm{p}(n)}) < \theta. \tag{6}$$

At any transmit interval, the following are probable:

1) None of $y_{\mathrm{p}(n)}$ and $y^{\dagger}_{\mathrm{p}(n)}$ are affected by IN,
2) Both $y_{\mathrm{p}(n)}$ and $y^{\dagger}_{\mathrm{p}(n)}$ are affected by IN,
3) Either $y_{\mathrm{p}(n)}$ or $y^{\dagger}_{\mathrm{p}(n)}$ is affected by IN.

If '1' is used to indicate that a symbol was affected by IN, while '0' indicates otherwise, then an IN error table can be represented as a logic AND truth table shown in Table 1. From Table 1, we observe that transmitting a copy of the information symbol in the form of its complex conjugate

TABLE 1. Impulse noise error probabilities on the received signal components from PLC.

$y_{\mathrm{p}(n)}$	$y^{\dagger}_{\mathrm{p}(n)}$	Output	Symbol recovery (Yes/No)
0	0	0	Yes
0	1	0	Yes
1	0	0	Yes
1	1	1	No

contributes to the $\frac{3}{4}$ outcomes when the output is '0'. Since, either $y_{\mathrm{p}(n)}$ or $y^{\dagger}_{\mathrm{p}(n)}$ can be selected for re-transmission at the VLC section, the probability of transmitting IN affected data symbols, is drastically reduced by 75%. In instances when both $y_{\mathrm{p}(n)}$ and $y^{\dagger}_{\mathrm{p}(n)}$ are affected by IN noise, then $y_{\mathrm{p}(n)}$ is clipped to zero, to avoid transmitting signals with higher peaks which could increase the PAPR.

B. PERMUTATION CODED TIME-DIVERSITY HERMITIAN SYMMETRY (PC-TDHS) BASED HPV SYSTEM

Since IN occurs in short random bursts, then spacing the information carrying time-slots can be another method to enhance the robustness of the system against IN. In light of this, a permutation coded TDHS (PC-TDHS) scheme is introduced to enhance the reliability of the HPV system. A further reduction in the complexity of the system is implemented by the use of an SD decoder. This decoder can be a better alternative to the hard-decision (HD) decoder whose computational complexity increases exponentially with an increase in the code length and cardinality, as shown in [55]. It is noted that the implementation of the PC-TDHS scheme reduces the spectral efficiency of the system. However, for applications where a trade-off between reliability and data-rate is tolerated, the PC-TDHS based system is a potential candidate.

A permutation code $\boldsymbol{P}$ consists of $|\boldsymbol{P}|$ codewords, each of length M. All $|\boldsymbol{P}|$ codewords in $\boldsymbol{P}$ are row vectors consisting of M different integers $1, 2, \ldots, M$, as symbols and denoted in this work by $\boldsymbol{v}_p$, where $p = 1, 2, \ldots, |\boldsymbol{P}|$. We use the notation $\mathcal{PC}(M, d_{\min})$ to describe $\boldsymbol{P}$ with minimum Hamming distance $d_{\min}$. Hence, $b = \lfloor \log_2 |\boldsymbol{P}| \rfloor$ bits are mapped per $\boldsymbol{v}_p$, where $\lfloor . \rfloor$ denotes the floor function. Note that the Hamming distance is the number of positions in which any codeword pair differs. Consequently, $d_{\min}$ is defined as the smallest Hamming distance between any codeword pairs in $\boldsymbol{P}$. In the PC-TDHS scheme, a sequence of N time-slots are divided into G groups of M time-slots and only one of the M time-slots in each group, is selected to carry information symbols. This has the potential to mitigate IN noise which occurs in short bursts, because the probability of IN affecting an information symbol in a group of M time-slots is $\frac{1}{M}$.

Information symbols consisting of b message bits have a one-to-one mapping with one of $|\boldsymbol{P}|$ codewords. Each information symbol with b bits is repeated over all the selected time-slots in the $\frac{G}{2}$ groups. Further, $\frac{G}{2} \cdot \mathcal{Q}$ bits can be modulated and $\mathcal{Q}$ bits assigned to each selected time-slot in each of the $\frac{N}{2}$ groups. Therefore, the total number of bits $\mathcal{B}_{\mathrm{t}}$ per

transmission period is

$$\mathcal{B}_t = \log_2 |\boldsymbol{P}| + \frac{G}{2} \cdot \mathcal{Q}. \tag{7}$$

Let $g = 1, 2, \ldots, \frac{G}{2}$ denote the different groups consisting of M time-slots, and let $l = 1, 2, \ldots, M$ denote the different time-slots in group g. It is worth noting that $M = \frac{G}{2}$, therefore, $g = 1, 2, \ldots, M$. Thus, the vector $\boldsymbol{x}_{\mathrm{p}}$ denoting the symbols to be transmitted via the PLC channel in the PC-TDHS scheme is

$$\boldsymbol{x}_{\mathrm{p}} = \underbrace{0 \ldots x_{\mathrm{p}_{1l}} \ldots 0}_{\text{Group 1}}, \underbrace{0 \ldots x_{\mathrm{p}_{2l}} \ldots 0}_{\text{Group 2}}, \ldots, \underbrace{0 \ldots x_{\mathrm{p}_{(G/2)l}} \ldots 0}_{\text{Group G/2}}. \tag{8}$$

In the TDHS scheme, the complex conjugate elements, $x^*{}_{\mathrm{p}_{gl}}$, of vector in (8) are generated to occupy the other $\frac{N}{2}$ time-slots, forming an HS structure. The transmission process till the VLC receiver is similar to that described in Section III-A.

Considering (3) and the structure of (8), we can express the received signal at the VLC receiver of the PC-TDHS HPV system after the FFT operation, as a matrix $\boldsymbol{Y}_{\mathrm{v}} = [(y_{\mathrm{v}})_{gl}] \in \mathcal{C}^{M \times M}$, where g and l will denote the rows and columns in the matrix. As in the uncoded TDHS system, maximum likelihood detection is used to estimate the constellation vector $\hat{\boldsymbol{x}}_{\mathrm{v}}$. If HD is used along with a threshold detector, then a threshold value τ to which the received signal is subjected to, is set. Consequently,

$$(\hat{y}_{\mathrm{v}})_{gl} = \begin{cases} 1, & \text{if } |(y_{\mathrm{v}})_{gl}| \geq \tau, \\ 0, & \text{otherwise}, \end{cases} \tag{9}$$

where $(\hat{y}_{\mathrm{v}})_{gl} = 0$ and $(\hat{y}_{\mathrm{v}})_{gl} = 1$ is an indication of inactive and active time-slots in each group. Each $\boldsymbol{v}_p \in \boldsymbol{P}$ can be converted to an equivalent $[0, 1]^{M \times M}$ codeword matrix $\boldsymbol{C}_p = [c_{gl}]$ such that in each column of $\boldsymbol{C}_p$, a '1' fills the position which corresponds to the codeword's integer, while other $M - 1$ values in the column are set to '0'. Therefore, the estimated matrix, $\hat{\boldsymbol{Y}}_{\mathrm{v}} = [(\hat{y}_{\mathrm{v}})_{gl}]^{M \times M} \in \{0, 1\}$, is compared with all likely $\boldsymbol{C}_p$ matrices at the receiver and then a decision is made based on the minimum distance.

1) PERMUTATION CODES AND SOFT-DECISION DECODING

When PCs are used, the low-complexity SD Hungarian-Murty (HM) decoder [55], [57], [58], can be used. In this type of decoder, the Hungarian algorithm solves an assignment problem, where the objective is to assign a number of resources to an equal number of activities [59]. Thus, minimising the total cost or maximising the total profit by such an allocation. The Hungarian algorithm assigns a job to each worker such that a worker can only be assigned one task. Thus, when the Hungarian algorithm is applied to a permutation coded communication system, the aim will be to find the optimal solution of the cost of the likely transmitted permutation codeword. The mathematical model of an assignment problem [55], [58], [59], can be expressed as:

$$K = \sum_{g=1}^{M} \sum_{l=1}^{M} c_{gl} |(y_{\mathrm{v}})_{gl}|, \tag{10}$$

subject to the constraints $\sum_{g=1}^{M} c_{gl} = \sum_{l=1}^{M} c_{gl} = 1$, $(g, l = 1, 2, \ldots, M)$, where K in (10) is the cost of the assignment and $|(y_{\mathrm{v}})_{gl}|$ denotes the cost of assigning a resource to an activity. From the model in (10), the Hungarian algorithm of the HM decoder iteratively finds an $M \times M$ matrix $\boldsymbol{R} = [r_{gl}] \in \mathbb{R}$ that produces the maximum cost K corresponding to $\boldsymbol{v}_p$. If the produced codeword is $\boldsymbol{v}_p \in \boldsymbol{P}$, then the decoder stops and the produced codeword is assumed to be the transmitted codeword. However, if the produced codeword does not belong to $\boldsymbol{P}$, then from $\boldsymbol{R}$, using the Murty's algorithm, the decoder finds the next highest $\mathcal{K}$ costs and ranks them in order of decreasing cost. The highest ranking cost corresponding to one of $\boldsymbol{v}_p \in \boldsymbol{P}$, is then selected to be the transmitted codeword. The HM decoding algorithm can be summarised and presented as follows:

Algorithm 1 HM Decoding in PC-TDHS Based HPV System

Input: Channel output matrix $\boldsymbol{Y}_{\mathbf{v}}$ in
Output: Permutation codeword $\boldsymbol{v}_p$ out
By Hungarian method, find matrix $\boldsymbol{R} = [r_{gl}] \in \mathbb{R}$
if $\boldsymbol{v}_p \in \boldsymbol{P}$ **then**
$\boldsymbol{v}_p$ is the transmitted permutation codeword
Stop decoder process
▷ Complexity order of $O(M^3)$ [60]
else
By Murty's algorithm, find the best $\mathcal{K}$ permutation codewords and rank them in order of increasing cost.
Select $\boldsymbol{v}_p$ corresponding to the highest ranking cost as the transmitted codeword
▷ Complexity order of $O(M^4)$ [61]
end if
▷ Overall worst case decoder complexity order is $O(M^4)$

C. MULTIPLE ACCESS FOR PC-TDHS BASED HPV SYSTEM

The PC-TDHS based HPV is the basis for the implementation of an MA scheme over a TDHS HPV system shown in Fig. 4. Simultaneous transmission from multiple users may compromise the gains of the single user PC-TDHS based system, however the spectral efficiency of an MA is enhanced as multiple users are able to access the channel. In an MA scheme, disjoint codebooks are assigned to multiple users, whereby information bits from users are mapped to specific codewords in their respective codebooks. The codewords in turn determine the specific time-slot to carry the modulated symbols, similar to the PC-TDHS scheme.

The computational complexity at the receiver increases exponentially when HD decoders are used. Hence, for reduced decoding complexity at the VLC receiver, we employ

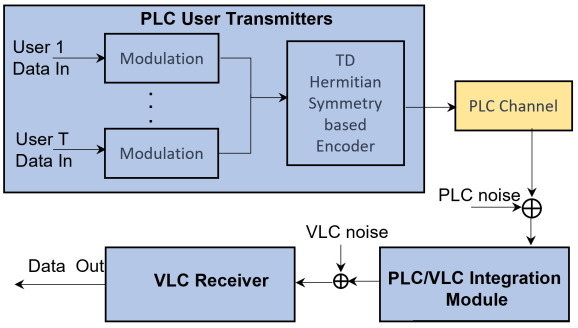

FIGURE 4. Block diagram for TDHS MA HPV Communication System.

the SD decoder based on the Hungarian and Murty's algorithms as presented in [55], whose decoding process differs only slightly compared to the description in Section III-B1. The difference is that when applied to an MA system, the decoder not only selects one best optimal solution from Murty's ranking, but the highest ranked m solutions, where m denotes the number of allowed active users.

In the system block diagram of the PC-TDHS based MA HPV system shown in Fig. 4, each user is assigned a set of codewords forming the user codebook, $\boldsymbol{P}_u$, where $u = 1, 2, \ldots, T$ and T is the number of users in the network. The $b_u = \log_2(|\boldsymbol{P}_u|)$ bits from a user's sequence of message bits, are mapped to each codeword $\boldsymbol{v}_p(u) \in \boldsymbol{P}_u$, where $p = 1, 2, \ldots, (|\boldsymbol{P}_u|)$. Each integer symbol of the user's codeword indicates which time-slot is activated for data transmission.

Assuming block synchronisation of the participating users, the users' input signals are added together forming what is referred to as a composite signal, which is then passed to the TDHS encoder. An example of the time-slot activation pattern due to $m = 2$, is demonstrated in Fig. 5. For simplicity, in Fig. 5, the subscripts denote the user number and integer positions of the respective user codewords. For instance, in v_{ul}, u is the user number while l the integer position. Additionally, v_{ul}, v_{ul} indicates that both users used the same time-slot number for transmission. The TDHS encoder arranges the composite signal in an HS structure before transmission to the PLC/VLC integrator module, via the PLC channel. For unique decodability by the HM SD decoder at the receiver, the minimum Hamming distance between codeword of different users and the cyclic properties of the combined permutation codewords, are cardinal.

The output signal vector, $\boldsymbol{y}_{\mathrm{p}}$, from the PLC channel affected by the channel noise is given as:

$$\boldsymbol{y}_{\mathrm{p}} = \sum_{u=1}^{m} \boldsymbol{x}_{\mathrm{p}}^{u} e^{j\phi} + \boldsymbol{n}_{\mathrm{p}}, \quad u = 1, 2, \ldots, m, \tag{11}$$

where $\boldsymbol{x}_{\mathrm{p}}^{u}$ is a vector consisting of the complex input information symbols from user u in the composite transmitted signal. As in (2), $\boldsymbol{n}_{\mathrm{p}} = \boldsymbol{n}_{\mathrm{G}} + \boldsymbol{n}_{\mathrm{I}}\sqrt{D}$ is the noise component in the PLC channel comprising the background noise $\boldsymbol{n}_{\mathrm{G}}$ modelled as AWGN with zero-mean and variance of $\sigma_{\mathrm{G}}^2 = 2N_0$ and the IN $\boldsymbol{n}_{\mathrm{I}}$ which follows a Poisson distribution and has a variance σ_{G}^2/A. At the PLC/VLC integration module, the process described in Section III-A, regarding IN detection and making the signal IM/DD compatible, is applied.

IV. SIMULATION RESULTS AND ANALYSIS

On the VLC section, an indoor environment is considered. The transmitter is placed in a downward orientation at 3.0 m above the floor, and the receiver is at 0.85 m above the floor, directly under the transmitter, in an upward orientation. In all the simulations, OFDM modulation is used at the VLC section and an array of $N = 32$ time-slots and sub-carriers are assumed for the PLC and VLC sections respectively. In addition, quadrature amplitude modulation (QAM), precisely 4-QAM, is used. For all coded systems, we apply a permutation codebook defined by $\mathcal{PC}(M = 4, d_{\min} = 3)$. Simulations for various system scenarios are conducted to obtain the BER and goodput performances versus the electrical signal-to-noise ratio (SNR) and a fixed optical SNR of 55 dB. Precisely, the following are simulated:

1) The HPV system where the TDHS scheme is not applied; this is referred to as the conventional or non-TDHS HPV system.
2) The TDHS-based HPV system.
3) The permutation coded non-TDHS and TDHS HPV systems denoted as PC non-TDHS and PC TDHS, respectively; employing HD and SD decoding techniques. While the AF protocol is applied in all the above mentioned systems, we additionally simulate a PC non-TDHS system employing the DF protocol.
4) A multiple-access PC-TDHS HPV system.

A. IMPACT OF IMPULSE NOISE ON SYSTEM PERFORMANCE

The effect of both the PLC and VLC channels on the transmitted signal, is considered. As such the system probability of error must be calculated accordingly; that is considering the probability of error due to the PLC channel, $P_{e,\mathrm{PLC}}$ and the probability of error due to the VLC channel, $P_{e,\mathrm{VLC}}$. Thus, the probability of error for the conventional HPV system (non TDHS), $P_{e,\text{non-TDHS}}$ can be expressed as:

$$P_{e,\text{non-TDHS}} = 1 - (1 - P_{e,\mathrm{PLC}}) \cdot (1 - P_{e,\mathrm{VLC}}). \tag{12}$$

As provided in [62],

$$P_{e,\mathrm{PLC}} = \gamma T_{\text{noise}} P_{e,\mathrm{I}} + (1 - \gamma T_{\text{noise}}) P_{e,\mathrm{B}}. \tag{13}$$

In (13), γ and T_{noise} denote the arrival rate and average duration of IN, while $P_{e,\mathrm{B}} = \frac{1}{2}\mathrm{erfc}\left(\sqrt{\frac{E_b}{N_0}}\right)$ is the probability of error when 4-QAM is considered [63]. The complementary error function is denoted by erfc(·), while E_b and N_0 denote the signal and noise power, respectively. Similarly, $P_{e,\mathrm{I}} = \frac{1}{2}\mathrm{erfc}\left(\sqrt{\frac{E_b}{N_0+N_i}}\right)$, is the probability of error in the presence of IN, where N_i denotes the IN power spectral density (PSD). The probability of error due to AWGN on a 4-QAM OFDM

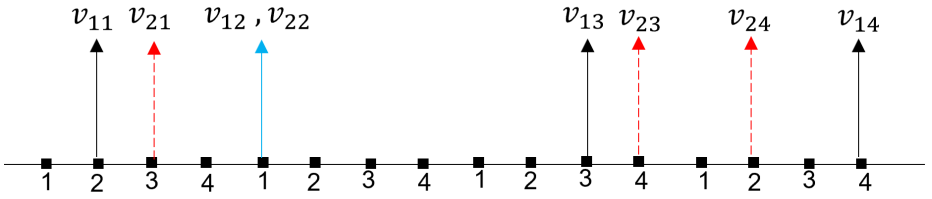

FIGURE 5. Time-slot activation representation in an MA PC-TDHS HPV system. User information symbols for two users mapped to user permutation codewords 2134 and 3142 for the two users.

modulated signal over the VLC channel is expressed as [63]:

$$P_e = \frac{1}{2}\text{erfc}\left(\sqrt{\frac{2\sqrt{N}-1}{2^{\sqrt{N}-1}}\cdot\frac{h\cdot E_b}{N_0}}\right), \tag{14}$$

where N denotes the number of OFDM sub-channels.

When the TDHS scheme is considered, the impact of the IN detector in the PLC-VLC integration unit, on the system error probability is accounted for. Thus,

$$P_{e,\text{TDHS}} = 1-(1-\Omega P_{e,\text{PLC}}^2)\cdot(1-P_{e,\text{VLC}}), \tag{15}$$

where Ω is a parameter that accounts for the performance of IN detection, whereby its performance in low SNR regions, is better than in high SNR regions. Thus, $\Omega \geq 1$, changes according to the SNR.

The system performance in terms of BER as a function of the SNR, was simulated. The varying values of A of 0.1, 0.05 and 0.01 were used in the computations. These varying A-values could depict different times of the day or different events in a day, inducing varying levels of IN in terms of the frequency of occurrence. Theoretical performances for both the conventional and the TDHS HPV systems are presented for validation of the simulations results. The impact of the proposed time-diversity scheme with an IN detector at the PLC/VLC integration section is evident in the TDHS theoretical BER curves. The effect of the IN is reduced and the background noise becomes dominate. Hence, as shown in Fig. 6, the error probability curve of the TDHS theoretical model shows a reduced error floor section.

An observation of superior performance for higher A-values is evident with increasing SNR values. This demonstrates a fundamental phenomena of IN occurrence, where a high value of A corresponds to low amplitude pulses with frequent occurrences, while a low value of A corresponds to high amplitude and less frequent pulses [64]. For all the A-values, the performance of the TDHS scheme is compared with that of the conventional system. For both theoretical and simulated results, Fig. 6, shows that the TDHS based systems, perform better than the conventional system. For instance, an SNR gain of 5 dB between the theoretical plots is noticed at a BER of 10^{-4}, where $A = 0.05$. Accordingly SNR gains for the simulated TDHS and conventional systems are 6 dB for $A = 0.01$, 5 dB for $A = 0.05$ and 4 dB for $A = 0.1$. The robustness of the TDHS based system is attributed to the transmission time diversity between the original data symbol

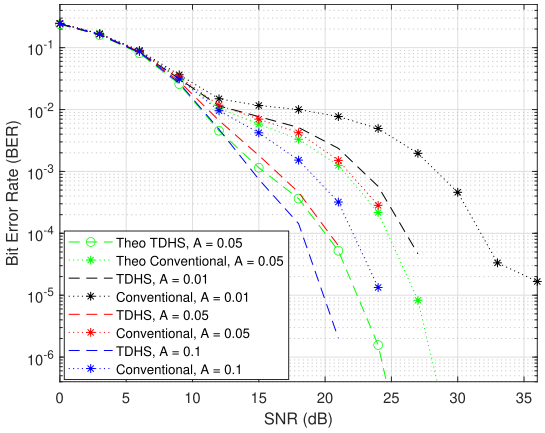

FIGURE 6. BER performance for TDHS and non-TDHS system for varying values of *A*.

and its complex conjugate component, as well as the fact that each copy of the information symbol has an independent probability of being affected by a different IN event. As demonstrated in Section III-A, the implementation of the TDHS scheme offers a 75% reduction in the probability of the data symbol being affected by IN. The performance shown in Fig. 6 demonstrates the effectiveness of the proposed TDHS scheme for IN mitigation in HPV systems.

B. BER PERFORMANCE COMPARISON BETWEEN UNCODED TDHS AND PC-TDHS SINGLE USER HPV SYSTEMS USING HD AND SD DECODERS

We further compare the BER performances of the TDHS uncoded system to that of TDHS coded (PC TDHS) system using the HD decoder. Despite the reduction in spectral efficiency, a superior BER performance of the PC-TDHS based system over the uncoded TDHS system is noticed, at higher SNR values. Precisely an SNR gain of 2 dB is achieved at a BER of 10^{-4}. This performance enhancement is due to the feature that the permutation code introduces in the time-slot activation pattern, where only some time-slots are activated to carry the modulated information bits. As a result the probability of the IN effect on the activated time-slot is reduced.

The performance of the coded TDHS HPV system is further enhanced in terms of reliability and decoding computation reduction by the use of the HM-based SD decoder.

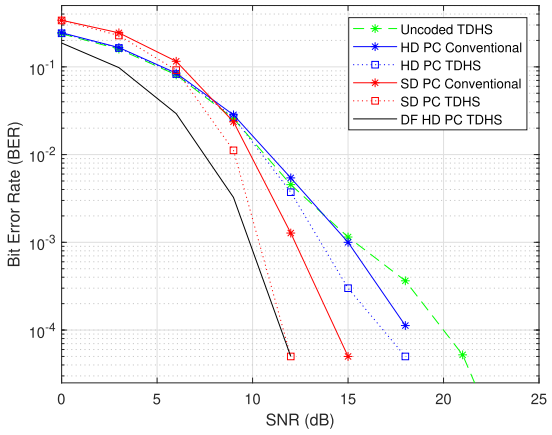

FIGURE 7. BER performance comparison between TDHS and Non-TDHS based HPV systems for coded and uncoded schemes. $A = 0.05$, $M = 4$ for coded systems.

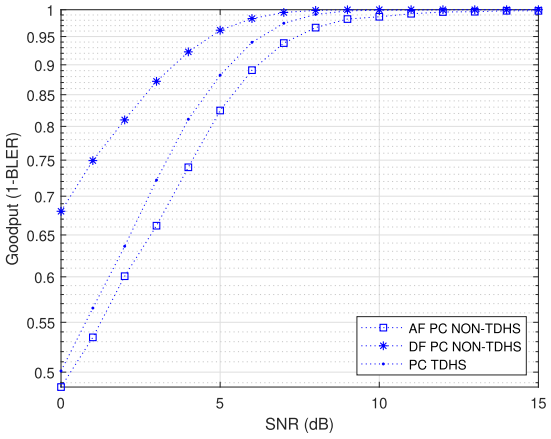

FIGURE 8. Goodput performance comparison for coded TDHS and non-TDHS systems employing AF and DF relaying protocols. SD decoding was used for all the systems.

In Fig. 7, the superior performance influenced by the HM SD decoder is noted when a coded conventional system is compared with the coded TDHS system using the HD decoder. Considering the positive effect of the HM decoder on the coded non-TDHS system, it is conceived that a combination of the TDHS scheme and the HM decoder on a coded system will provide further performance enhancement. Suffice to say, the BER performance of a PC-TDHS HPV system using the HM SD decoder, is also shown in Fig. 7, with an enhanced performance over the PC non-TDHS system using the same the HM decoder, and the TDHS system using the HD decoder.

C. PERFORMANCE COMPARISON BETWEEN HPV SYSTEMS EMPLOYING AMPLIFY-AND-FORWARD (AF) AND DECODE-AND-FORWARD (DF) RELAYING PROTOCOLS

All except one plot in Fig. 7 are results from HPV systems simulated with the AF relaying protocol. The exception shows the BER performance of the PC non-TDHS system employing the DF protocol. The superior performance of the DF-based non-TDHS over the TDHS systems is evident until a BER of 10^{-4}. As such, this translates into a superior goodput performance, as depicted in Fig. 8. In this work, the definition of the system goodput is given as the difference between the total transmitted data blocks and the block error rate (BLER); where BLER is a ratio of the number of erroneous blocks to the total number of blocks transmitted. Thus, we express goodput as $1 - \text{BLER}$. The superior performance of the non-TDHS HPV system using the DF relaying protocol over the TDHS system, is due to the fact that information received from the PLC channel is only forwarded to the destination if the decoding is deemed successful by the error detection code. However, the enhanced performance over AF enabled schemes is achieved at higher computational complexity. While the TDHS scheme using the AF relaying protocol only detects if the transmitted data was affected by IN with a complexity of $O(M^2)$, the DF scheme as seen in Fig. 9 requires several signal processes

TDHS AF System Processes	Non-TDHS DF System Processes
Encode and Modulation	
Hermitian symmetry	-
PLC Channel	
-	Demodulate
IN detection $\min(y_n, y_n^{\dagger}) < \theta$ Complexity: $O(M^2)$	Decoding with complexities: $O(M^4)$ for SD $O(M!\,M^2)$ for HD.
-	Encode
-	Modulate
Signal preparation for transmission via VLC channel	

FIGURE 9. Comparison of major signal processes between TDHS system using the AF relaying protocol and non-TDHS system using the DF relaying protocol. Grey portions depict common processes, while white portions indicate processes not applicable to a particular system. Blue and orange portions depict processes applicable only to either the TDHS or the non-TDHS system, respectively.

before re-transmission to the VLC receiver. In addition to the computational complexities of the demodulation, encoding and modulation of the considered coded system, the decoding complexities are $O(M^4)$ and $O(M! \cdot M^2)$ for SD and HD decoding, respectively [55]. Moreover, the performance of the PC-TDHS system using the HM decoder improves and is comparaable to the DF-based TDHS system. Therefore, the proposed TDHS scheme would be a cost-effective option.

D. BER PERFORMANCE PC-TDHS BASED MA HPV SYSTEMS

The BER performance of the TDHS based MA HPV system using the HM decoder, is shown in Fig. 10. As expected, from the trend in Figs. 6 and 7, the PC TDHS MA HPV system outperforms that of the coded non-TDHS MA HPV system. For example, over 2 dB difference in SNR at 10^{-3} is noticed. Furthermore, since multiple time-slots are activated in each G group, the number of time-slots prone to the IN effect also increases. Hence, the single user PC-TDHS system also using the HM decoder, outperforms the system with MA scheme. However, the MA implementation increases the channel utilisation, thus a trade-off between the BER performance and the spectral efficiency is inevitable.

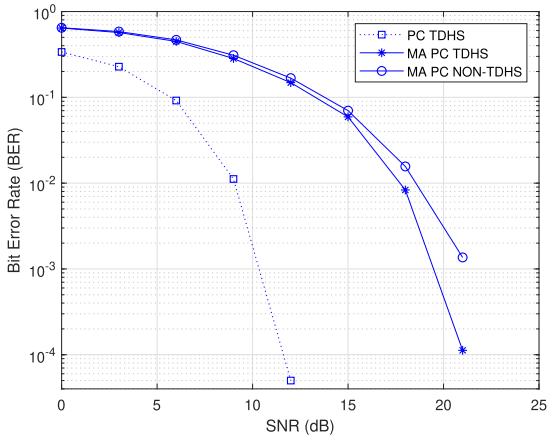

FIGURE 10. BER performance of the MA HPV system using the permutation coded TDHS. $A = 0.05$, $M = 4$, $m = 2$.

V. CONCLUSION

In this paper, an investigation on the reliability performance of a hybrid technology system identified to be critical for continued development of IoT, was conducted. Precisely, a novel scheme for IN mitigation in an HPV communication system has been presented. The scheme is based on a time-diversity concept that uses the Hermitian symmetry structure to introduce data repetition and recover information symbols that are likely to have been affected by IN. Thus, referred to as time-diversity Hermitian symmetry (TDHS) scheme for IN mitigation. The use of the TDHS scheme results in a 75% chance to recover IN affected data symbols at the PLC/VLC integration unit. In comparison to the conventional system, the TDHS-based HPV system has a better BER performance that is attributed to the fact that information symbols affected by IN could be recovered using their respective copies that are simultaneously transmitted with them, in complex conjugate form.

Further, the TDHS scheme was implemented over a permutation coded HPV system using soft decision decoding. Compared to the uncoded TDHS HPV system, the PC TDHS based system demonstrated enhanced reliability where an SNR gain of over 6 dB at a BER of 10^{-4} for both HD and SD decoders, was achieved. The use of the SD HM decoder with the TDHS scheme further improved the BER when compared to the one employing the HD decoder. Despite the poorer performance when compared to a PC conventional system using the DF protocol, the proposed TDHS based HPV system using the AF protocol has acceptable performance metrics in terms of BER and goodput, yet with a lower computational complexity. Furthermore, PCs provided a base for the implementation of a permutation coded MA HPV system whose decoding complexity is reduced by employing an SD HM decoder.

REFERENCES

[1] J. A. Stankovic, "Research directions for the Internet of Things," *IEEE Internet Things J.*, vol. 1, no. 1, pp. 3–9, Feb. 2014.

[2] A. Zanella, N. Bui, A. Castellani, L. Vangelista, and M. Zorzi, "Internet of Things for smart cities," *IEEE Internet Things J.*, vol. 1, no. 1, pp. 22–32, Feb. 2014.

[3] O. Kolade and L. Cheng, "Memory channel models of a hybrid PLC-VLC link for a smart underground mine," *IEEE Internet Things J.*, vol. 9, no. 14, pp. 11893–11903, Jul. 2022.

[4] M. Jani, P. Garg, and A. Gupta, "On the performance of a cooperative PLC-VLC indoor broadcasting system consisting of mobile user nodes for IoT networks," *IEEE Trans. Broadcast.*, vol. 67, no. 1, pp. 289–298, Mar. 2021.

[5] L. De M. B. A. Dib, V. Fernandes, M. de L. Filomeno, and M. V. Ribeiro, "Hybrid PLC/wireless communication for smart grids and Internet of Things applications," *IEEE Internet Things J.*, vol. 5, no. 2, pp. 655–667, Apr. 2018.

[6] Y. Sreenivasa Reddy, M. Panda, A. Dubey, A. Kumar, T. Panigrahi, and K. M. Rabie, "Optimisation of indoor hybrid PLC/VLC/RF communication systems," *IET Commun.*, vol. 14, no. 1, pp. 117–126, Jan. 2020.

[7] D. A. Basnayaka and H. Haas, "Hybrid RF and VLC systems: Improving user data rate performance of VLC systems," in *Proc. IEEE 81st Veh. Technol. Conf. (VTC Spring)*, May 2015, pp. 1–5.

[8] Q. W. Pan and A. Kathnaur, "Power-line networks to extend ranges of 2.4 GHz wireless communications inside multi-storey buildings," in *Proc. IEEE Radio Wireless Symp. (RWS)*, Jan. 2010, pp. 621–624.

[9] W. Zhu, X. Zhu, E. Lim, and Y. Huang, "State-of-art power line communications channel modelling," *Proc. Comput. Sci.*, vol. 17, pp. 563–570, Jan. 2013.

[10] T. Komine and M. Nakagawa, "Fundamental analysis for visible-light communication system using LED lights," *IEEE Trans. Consum. Electron.*, vol. 50, no. 1, pp. 100–107, Feb. 2004.

[11] Y. Tanaka, T. Komine, S. Haruyama, and M. Nakagawa, "Indoor visible communication utilizing plural white LEDs as lighting," in *Proc. 12th IEEE Int. Symp. Pers., Indoor Mobile Radio Commun. (PIMRC)*, vol. 2, Sep. 2001, pp. F–F.

[12] L. Lampe, A. M. Tonello, and T. G. Swart, *Power Line Communications: Principles, Standards and Applications From Multimedia to Smart Grid*. Hoboken, NJ, USA: Wiley, 2016.

[13] A. Camponogara, H. V. Poor, and M. V. Ribeiro, "The complete and incomplete low-bit-rate hybrid PLC/wireless channel models: Physical layer security analyses," *IEEE Internet Things J.*, vol. 6, no. 2, pp. 2760–2769, Apr. 2019.

[14] M. Shang, Q. Liu, and C.-Y. Sheu, "Foglight: Visible light-enabled indoor localization system for low-power IoT devices," *IEEE Internet Things J.*, vol. 5, no. 1, pp. 175–185, Feb. 2018.

[15] A. Bazzi, B. M. Masini, A. Zanella, and A. Calisti, "Visible light communications as a complementary technology for the internet of vehicles," *Comput. Commun.*, vol. 93, pp. 39–51, Nov. 2016.

[16] T. Komine and M. Nakagawa, "Integrated system of white LED visible-light communication and power-line communication," *IEEE Trans. Consum. Electron.*, vol. 49, no. 1, pp. 71–79, Feb. 2003.

[17] X. Ma, J. Gao, F. Yang, W. Ding, H. Yang, and J. Song, "Integrated power line and visible light communication system compatible with multi-service transmission," *IET Commun.*, vol. 11, no. 1, pp. 104–111, 2017.

[18] W. Ding, F. Yang, H. Yang, J. Wang, X. Wang, X. Zhang, and J. Song, "A hybrid power line and visible light communication system for indoor hospital applications," *Comput. Ind.*, vol. 68, pp. 170–178, Apr. 2015.

[19] S. M. Nlom, A. R. Ndjiongue, K. Ouahada, H. C. Ferreira, A. J. H. Vinck, and T. Shongwe, "A simplistic channel model for cascaded PLC-VLC systems," in *Proc. IEEE Int. Symp. Power Line Commun. Appl. (ISPLC)*, 2017, pp. 1–6.

[20] S. M. Nlom, A. R. Ndjiongue, and K. Ouahada, "Cascaded PLC-VLC channel: An indoor measurements campaign," *IEEE Access*, vol. 6, pp. 25230–25239, 2018.

[21] A. D. Familua, A. R. Ndjiongue, K. Ogunyanda, L. Cheng, H. C. Ferreira, and T. G. Swart, "A semi-hidden Markov modeling of a low complexity FSK-OOK in-house PLC and VLC integration," in *Proc. IEEE Int. Symp. Power Line Commun. Its Appl. (ISPLC)*, Mar. 2015, pp. 199–204.

[22] O. Kolade, A. D. Familua, and L. Cheng, "Indoor amplify-and-forward power-line and visible light communication channel model based on a semi-hidden Markov model," *AEU-Int. J. Electron. Commun.*, vol. 124, Sep. 2020, Art. no. 153108.

[23] H. Ma, L. Lampe, and S. Hranilovic, "Integration of indoor visible light and power line communication systems," in *Proc. IEEE 17th Int. Symp. Power Line Commun. Appl.*, Mar. 2013, pp. 291–296.

[24] M. S. A. Mossaad, S. Hranilovic, and L. Lampe, "Amplify-and-forward integration of power line and visible light communications," in *Proc. IEEE Global Conf. Signal Inf. Process. (GlobalSIP)*, Dec. 2015, pp. 1322–1326.

[25] K. Bhavya, N. Gangrade, and N. Kumar, "Simplified integration of power line and visible light communication," in *Proc. 3rd Int. Conf. Commun. Electron. Syst. (ICCES)*, Oct. 2018, pp. 129–132.
[26] M. Shimaponda-Nawa, S. Achari, D. N. K. Jayakody, and L. Cheng, "Visible light communication system employing space time coded relay nodes and imaging receivers," *SAIEE Afr. Res. J.*, vol. 111, no. 2, pp. 56–64, Jun. 2020.
[27] A. Kumar and S. K. Ghorai, "BER performance analysis of OFDM-based integrated PLC and MIMO-VLC system," *IET Optoelectron.*, vol. 14, no. 5, pp. 242–251, 2020.
[28] T. Komine, S. Haruyama, and M. Nakagawa, "Performance evaluation of narrowband OFDM on integrated system of power line communication and visible light wireless communication," in *Proc. 1st Int. Symp. Wireless Pervasive Comput.*, Jan. 2006, p. 6.
[29] A. R. Ndjiongue, H. C. Ferreira, and T. M. N. Ngatched, "Constellation design for cascaded MPSK-CSK systems," in *Proc. IEEE Int. Conf. Commun. Workshops (ICC Workshops)*, May 2017, pp. 17–22.
[30] J. Gao, F. Yang, and W. Ding, "Novel integrated power line and visible light communication system with bit division multiplexing," in *Proc. Int. Wireless Commun. Mobile Comput. Conf. (IWCMC)*, Aug. 2015, pp. 680–684.
[31] H. Ma, L. Lampe, and S. Hranilovic, "Hybrid visible light and power line communication for indoor multiuser downlink," *IEEE/OSA J. Opt. Commun. Netw.*, vol. 9, no. 8, pp. 635–647, Aug. 2017.
[32] S. Feng, T. Bai, and L. Hanzo, "Joint power allocation for the multi-user NOMA-downlink in a power-line-fed VLC network," *IEEE Trans. Veh. Technol.*, vol. 68, no. 5, pp. 5185–5190, May 2019.
[33] D. Teng, Y. Zheng, M. Luo, Y. Luo, and W. Jinyuan, "Joint user pairing and subcarrier allocation for NOMA-based hybrid power line and visible light communication systems," in *Proc. J. Phys., Conf.*, 2020, vol. 1693, no. 1, Art. no. 012159.
[34] D. Middleton, "Statistical-physical models of electromagnetic interference," *IEEE Trans. Electromagn. Compat.*, vol. EMC-19, no. 3, pp. 106–127, Aug. 1977.
[35] S. Galli and T. Banwell, "A novel approach to the modeling of the indoor power line channel—Part II: Transfer function and its properties," *IEEE Trans. Power Del.*, vol. 20, no. 3, pp. 1869–1878, Jul. 2005.
[36] A. M. Tonello, F. Versolatto, and A. Pittolo, "In-home power line communication channel: Statistical characterization," *IEEE Trans. Commun.*, vol. 62, no. 6, pp. 2096–2106, Jun. 2014.
[37] A. Rajesh and R. Nakkeeran, "Performance analysis of integrated system under impulse noise and multipath channel using turbo coded OFDM," in *Proc. 16th Int. Conf. Adv. Comput. Commun.*, Dec. 2008, pp. 254–259.
[38] L. Cheng and H. C. Ferreira, "Time-diversity permutation coding scheme for narrow-band power-line channels," in *Proc. IEEE Int. Symp. Power Line Commun. Appl.*, Mar. 2012, pp. 120–125.
[39] A. D. Familua and L. Cheng, "First and second-order semi-hidden Fritchman Markov models for a multi-carrier based indoor narrowband power line communication system," *Phys. Commun.*, vol. 29, pp. 55–66, Aug. 2018.
[40] T. Shongwe, A. H. Vinck, and H. C. Ferreira, "A study on impulse noise and its models," *SAIEE Afr. Res. J.*, vol. 106, no. 3, pp. 119–131, Sep. 2015.
[41] L. Di Bert, P. Caldera, D. Schwingshackl, and A. M. Tonello, "On noise modeling for power line communications," in *Proc. IEEE Int. Symp. Power Line Commun. Appl.*, Apr. 2011, pp. 283–288.
[42] S. V. Zhidkov, "Analysis and comparison of several simple impulsive noise mitigation schemes for OFDM receivers," *IEEE Trans. Commun.*, vol. 56, no. 1, pp. 5–9, Jan. 2008.
[43] K. M. Rabie and E. Alsusa, "Improving blanking/clipping based impulsive noise mitigation over powerline channels," in *Proc. IEEE 24th Annu. Int. Symp. Pers., Indoor, Mobile Radio Commun. (PIMRC)*, Sep. 2013, pp. 3413–3417.
[44] A. Mengi and A. J. Han Vinck, "Successive impulsive noise suppression in OFDM," in *Proc. ISPLC*, Mar. 2010, pp. 33–37.
[45] J. Häring and A. H. Vinck, "OFDM transmission corrupted by impulsive noise," in *Proc. Int. Symp. Power-Line Commun. Appl.*, Limerick, Ireland, 2000, pp. 5–7.
[46] B. Adebisi, K. M. Rabie, A. Ikpehai, C. Soltanpur, and A. Wells, "Vector OFDM transmission over non-Gaussian power line communication channels," *IEEE Syst. J.*, vol. 12, no. 3, pp. 2344–2352, Sep. 2018.
[47] A. Ikpehai, B. Adebisi, K. M. Rabie, M. Fernando, and A. Wells, "Energy-efficient vector OFDM PLC systems with dynamic peak-based threshold estimation," *IEEE Access*, vol. 5, pp. 10723–10733, 2017.
[48] K. M. Rabie, E. Alsusa, A. D. Familua, and L. Cheng, "Constant envelope OFDM transmission over impulsive noise power-line communication channels," in *Proc. IEEE Int. Symp. Power Line Commun. Appl. (ISPLC)*, Apr. 2015, pp. 13–18.
[49] B. Jamal and B. Ali, "Performance evaluation of CE-OFDM in PLC channel," *Signal Process., Int. J.*, vol. 4, no. 6, p. 318, 2011.
[50] A. Vinck, "Coded modulation for powerline communications," *Int. J. Electron. Commun.*, vol. 54, no. 1, pp. 45–50, 2000.
[51] A. J. H. Vinck, "Coding for a terrible channel," in *Proc. 2nd Workshop Special Topics 4G Technol. (EU-COST)*. Duisburg, Germany: Univ. Duisburg-Essen, Jul. 2005, pp. 101–106.
[52] O. Kolade and L. Cheng, "Impulse noise mitigation using subcarrier coding of OFDM-MFSK scheme in powerline channel," in *Proc. IEEE Int. Conf. Commun., Control, Comput. Technol. Smart Grids (SmartGridComm)*, Oct. 2019, pp. 1–6.
[53] O. Kolade, A. M. Abu-Mahfouz, and L. Cheng, "A subcarrier permutation scheme for noise mitigation and multi-access in powerline channels," in *Proc. IEEE Int. Symp. Power Line Commun. Appl. (ISPLC)*, Oct. 2021, pp. 19–24.
[54] M. Shimaponda-Nawa, O. Kolade, and L. Cheng, "Generalized permutation coded OFDM-MFSK in hybrid powerline and visible light communication," *IEEE Access*, vol. 10, pp. 20783–20792, 2022.
[55] M. Shimaponda-Nawa, O. Kolade, W. Ding, D. N. K. Jayakody, and L. Cheng, "Soft-decision decoding of permutation-based optical codes for a multiple access system," *IEEE Commun. Lett.*, vol. 25, no. 9, pp. 2824–2828, Sep. 2021.
[56] J. M. Kahn and J. R. Barry, "Wireless infrared communications," *Proc. IEEE*, vol. 85, no. 2, pp. 265–298, Feb. 1997.
[57] O. Kolade and L. Cheng, "Permutation-aided space-time shift keying for indoor visible light communication," in *Proc. IEEE Int. Conf. Commun., Control, Comput. Technol. Smart Grids (SmartGridComm)*, Oct. 2019, pp. 1–6.
[58] O. Kolade, J. Versfeld, and M. van Wyk, "Soft-decision decoding of permutation block codes in AWGN and Rayleigh fading channels," *IEEE Commun. Lett.*, vol. 21, no. 12, pp. 2590–2593, Dec. 2017.
[59] H. W. Kuhn, "The Hungarian method for the assignment problem," *Naval Res. Logistics Quarterly*, vol. 2, nos. 1–2, pp. 83–97, 1955.
[60] L. Liu and D. A. Shell, "Assessing optimal assignment under uncertainty: An interval-based algorithm," *Int. J. Robot. Res.*, vol. 30, no. 7, pp. 936–953, Jun. 2011.
[61] I. J. Cox, M. L. Miller, R. Danchick, and G. E. Newnam, "A comparison of two algorithms for determining ranked assignments with application to multitarget tracking and motion correspondence," *IEEE Trans. Aerosp. Electron. Syst.*, vol. 33, no. 1, pp. 295–301, Jan. 1997.
[62] O. Kolade, A. D. Familua, and L. Cheng, "Channel models for an indoor power line communication system," *IET-Commun. Technol. Netw. Smart Cities*, vol. 90, p. 67, Mar. 2021.
[63] J. van Wyk and L. Linde, "Bit error probability for a M-ary QAM OFDM-based system," in *Proc. AFRICON*, Sep. 2007, pp. 1–5.
[64] A. Hosseinpour Najarkolaei, W. Hosny, and J. Lota, "Bit error rate performance in power line communication channels with impulsive noise," in *Proc. 17th UKSim-AMSS Int. Conf. Modeling Simulation (UKSim)*, Mar. 2015, pp. 248–251.

MULUNDUMINA SHIMAPONDA-NAWA received the B.Eng. degree in electrical and electronics engineering from The Copperbelt University (CBU), Zambia, in 2008, the M.Ing. degree *(cum laude)* from the University of Johannesburg (UJ), South Africa, in 2015, and the Ph.D. degree in electrical and information engineering from the University of the Witwatersrand Johannesburg, South Africa, in 2022. Prior to that, she worked at Airtel Zambia as a Transmission Planning Engineer and the Team Leader, designing and optimizing the Telco's transport network. She is currently a Postdoctoral Research Fellow at the Faculty of Engineering and Built Environment (EBE), Wits Mining Institute (WMI), University of the Witwatersrand Johannesburg. Her research interests include visible light communications (VLC), powerline communications (PLC), optical fiber communications (OFC), and information management systems for the mining industry.

OLUWAFEMI KOLADE received the Ph.D. degree from the University of the Witwatersrand (Wits), South Africa. He is currently a Postdoctoral Research Assistant at the Department of Meteorology, University of Reading, U.K. Prior to this, he was a Postdoctoral Associate in smart grid research at Wits. His research interests include the implementation of data assimilation algorithms for climate and weather prediction, signal processing, error correction, and machine learning for communication channels.

JIANHUA HE (Senior Member, IEEE) received the Ph.D. degree from Nanyang Technological University, Singapore, in 2002. He is currently a Reader with the University of Essex, U.K. Before joining the University of Essex, he worked at the University of Bristol, Swansea University, and Aston University. He has published more than 150 research papers in refereed international journals and conferences. His research interests include 5G/6G wireless communications and networks, connected vehicles, autonomous driving, the Internet of Things, mobile edge computing, intelligent transport systems, data analytics, AI, and machine learning. He was the Workshop Chair of MobiArch'20 and ICAV'21, a Steering Committee Member of MobiArch'21, and a member of editorial board for several international journals. He is also the Coordinator of EU Horizon2020 projects COSAFE and VESAFE on cooperative connected autonomous vehicles.

WENBO DING (Member, IEEE) received the B.S. and Ph.D. degrees (Hons.) from Tsinghua University, in 2011 and 2016, respectively. He worked as a Postdoctoral Research Fellow at Georgia Tech under the supervision of Professor Z. L. Wang, from 2016 to 2019. He is currently a Tenure-Track Assistant Professor and a Ph.D. Supervisor at the Tsinghua Shenzhen International Graduate School, Tsinghua-Berkeley Shenzhen Institute, Tsinghua University, where he leads the Smart Sensing and Robotics (SSR) Group. His research interests include diverse and interdisciplinary, which include self-powered sensors, energy harvesting, and wearable devices for health and soft robotics with the help of signal processing, machine learning, and mobile computing. He has received many prestigious awards, including the Gold Medal of the 47th International Exhibition of Inventions Geneva and the IEEE Scott Helt Memorial Award.

LING CHENG (Senior Member, IEEE) received the B.Eng. degree *(cum laude)* in electronics and information from the Huazhong University of Science and Technology (HUST), in 1995, and the M.Ing. degree *(cum laude)* in electrical and electronics and the D.Ing. degree in electrical and electronics from the University of Johannesburg (UJ), in 2005 and 2011, respectively. In 2010, he joined the University of the Witwatersrand, where he was promoted to a Full Professor, in 2019. His research interests include telecommunications and artificial intelligence. He serves as an associate editor for three journals. He has published more than 100 research papers in journals and conference proceedings. He has been a visiting professor at five universities and the principal advisor for over 40 full research master's students. He was awarded the Chancellor's medals, in 2005 and 2019, and the National Research Foundation ratings, in 2014 and 2020. The IEEE ISPLC 2015 best student paper award was made to his Ph.D. student in Austin. He is the Vice-Chair of IEEE South African Information Theory Chapter.